Roles of donor and acceptor nanodomains in 6% efficient thermally annealed polymer photovoltaics

Kyungkon Kim, Jiwen Liu, Manoj A. Namboothiry, and David L. Carroll

Citation: Appl. Phys. Lett. **90**, 163511 (2007); doi: 10.1063/1.2730756
View online: http://dx.doi.org/10.1063/1.2730756
View Table of Contents: http://apl.aip.org/resource/1/APPLAB/v90/i16
Published by the American Institute of Physics.

Roles of donor and acceptor nanodomains in 6% efficient thermally annealed polymer photovoltaics

Kyungkon Kim
Materials Science and Technology Division, Korea Institute of Science and Technology, Seoul 136-791, Korea

Jiwen Liu, Manoj A. G. Namboothiry, and David L. Carroll[a)]
Center for Nanotechnology and Molecular Materials, Department of Physics, Wake Forest University, Winston-Salem, North Carolina 27109

(Received 4 March 2007; accepted 26 March 2007; published online 19 April 2007)

The authors have fabricated thin film polymer photovoltaics using 1-(3-methoxycarbonyl)propyl-1-phenyl-(6,6)C61 within regioregular poly(3-hexylthiophene) bulk heterojunction absorbing layers. Using thermal annealing at temperatures approaching the glass transition temperature, they have examined the formation of nanodomains within the matrix. These domains modify charge transport pathways in such a way as to allow for the efficient use of thicker absorbing layers. This results in a nearly 20% gain in overall performance for this polymer system with external power efficiencies exceeding 6%. © *2007 American Institute of Physics*. [DOI: 10.1063/1.2730756]

Research into conjugated polymers for photovoltaic (PV) devices has seen exciting growth over the past couple of years as developments in organic synthesis and device fabrication techniques have continued to raise power conversion efficiencies.[1] Recently, we have reported PV efficiencies of ~5%, corroborated by several other research groups, using thermal annealing of poly-3-hexylthiophene (P3HT)/soluble C_{60} (PCBM) bulk heterojunction (BHJ) system at temperatures near the glass transition (T_g), of P3HT.[2–5] This result has stimulated debate as to the role of the domain structure in the BHJ nanophase and the degree of crystallization in the host polymer.

P3HT is semicrystalline at room temperature.[6] There are two possibilities on how a nanophase material such as PCBM introduced into this matrix might influence its crystallization. If the PCBM is introduced as relatively large aggregates of crystallites, the crystallization of P3HT may be hindered. Alternatively, should the PCBM be well dispersed (small crystallites or individual molecules) when introduced into the polymer surface energy effects may induce heterogenous nucleation of crystallization of the polymer, as seen in the case of carbon nanotubes.[7] Thus, it is reasonable to believe that the initial dispersion properties of the nanophase within the polymer will influence the crystallization of the polymer phase. For good initial dispersions of the nanophase, we therefore expect the P3HT in the unannealed BHJ devices to be less crystalline than that in annealed BHJ devices. As a result π-π overlap between main chains increases when the devices are annealed, resulting in a redshift of the P3HT absorption maximum as observed.[6] Further, during annealing and polymer crystallization, phase separation between P3HT and PCBM occurs. This forms nanodomains of crystallized polymer and nanowhiskers of PCBM, as discussed in our previous work.[8]

In this letter, we suggest that morphological changes in the nanophase dispersant *and* in the polymer, as described above, lead to modifications in conduction mechanisms for the annealed systems. This allows for a more efficient use of thicker absorbing layers in devices.

The preparation procedures and fabrication of our bulk heterojunction photovoltaic devices (BHJ PV devices) are reported in our previous work.[2] For this study, three sets of devices were fabricated. We begin with glass/indium tin oxide (Delta Technologies $R_s = 10\ \Omega\ \mathrm{sq}^{-1}$) substrates. Poly(3,4-ethylenedioxythiophene):poly(styrenesulfonate) (PEDOT:PSS) (Baytron P) was deposited by spin coating at 4000 rpm and dried at 80 °C for 10 min. For device set 1 (D1), 12 mg of P3HT ($M_w \sim 48\,000$) was dissolved in 1 ml of chlorobenzene, filtered with a 0.2 μm filter, and blended with PCBM in ratio of 1:0.6 polymer to PCBM by weight. The composite material was spin coated onto the PEDOT:PSS layer at 1500 rpm. For device set 2 (D2), 15 mg of P3HT ($M_w \sim 48\,000$) was dissolved in 1 ml of chlorobenzene, filtered with a 0.2 μm filter, and blended with PCBM in ratio of 1:0.6 polymer to PCBM by weight. The composite material was spin coated onto the PEDOT:PSS layer at 1500 rpm. Finally, device set three (D3), 15 mg of P3HT ($M_w \sim 48\,000$) was dissolved in 1 ml of chlorobenzene, filtered with a 0.2 μm filter, and blended with PCBM in ratio of 1:0.6 polymer to PCBM by weight. The composite material was spin coated onto the PEDOT:PSS layer at 1200 rpm. The absorption profiles of these films annealed at 158 °C are shown in Fig. 1(a).

Lithium fluoride (LiF) (Aldrich) and aluminum (Al) (Sigma-Aldrich) electrodes were deposited via thermal evaporation at approximately 3–4 Å and 100 nm thick, respectively. The LiF was exposed to H_2O as described in literature before the Al deposition.[9] The active area of these devices is between 5 and 10 mm^2. The devices were encapsulated in a dry nitrogen glovebox and annealed using direct contact with a hot plate at 158 °C for 8 min.

A comparison of annealed films, for the D1 devices, using transmission electron microscopy (TEM) is shown in Figs. 1(b) and 1(c). We interpret these images to show what dark PCBM domains forming after annealing, consistent

a)Author to whom correspondence should be addressed; electronic mail: carroldl@wfu.edu

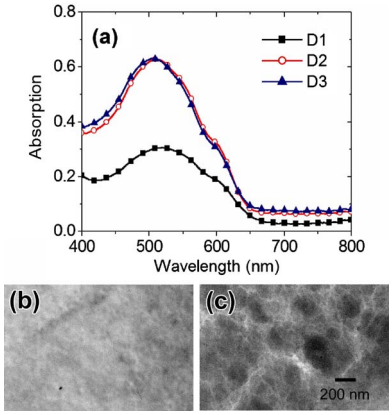

FIG. 1. (Color online) (a) Absoprtion spectra of annealed P3HT:PCBM blend films for D1, D2, and D3. Transmission electron microscopy pictures of the D1 P3HT:PCBM film (b) before annealing and (c) after annealing.

with our previous reports using atomic force microscopy combined with TEM. Results from thicker films are similar (not shown).[8]

As we and other groups have confirmed, these domains are themselves relatively crystalline.[3,8,10] Crystalline PCBM domains together with the crystalline P3HT as the absorbing layer will have two effects on the device's performance. The first is that they will provide facile charge separation and transport from the photoexcitation of PCBM and P3HT because across such domains there is little hopping conductivity. Secondly, the maximum optical absorption of the annealed P3HT:PCBM increases for the annealed system. That is, for a given thickness of film, the more crystalline the polymer, the greater its ability to absorb light.

To understand the effects of nanodomain formation on device performance as a function of spectral response, the external quantum efficiency (EQE) was determined for both the annealed (PV-H) and unannealed (PV-NH) D1 devices. Again, results for the D2 and D3 devices are similar. The EQE spectra are compared in Figs. 2(a)–2(d). Since the conduction in these devices is dominated by hopping mechanisms, we show the spectra as a function of temperature. Enhancements in EQE can be understood through Eq. (1)

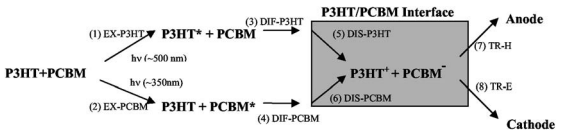

Equation (1). (1)

Excitons are generated from the photoexcitation of P3HT or PCBM [steps (1) and (2)] of Eq. (1) and migrate to the interface of P3HT/PCBM [steps (3) and (4)], followed by dissociation of electrons and holes through charge transfer [steps (5) and (6)]. Dissociated charge carriers are transported to the corresponding electrode [steps (7) and (8)].

Thus, the increased absorption in P3HT [step (1)], increased exciton migration length through forming the crystalline percolation path [steps (3) and (4)], and enhanced charge carrier transport [steps (7) and (8)] are thought to be the main reason for the EQE enhancement at 500 nm for the annealed devices over the unannealed.[11,12]

Notice that as the temperature is lowered, the overall response of both the annealed and unannealed devices decreases. This is likely to be because thermal activation of

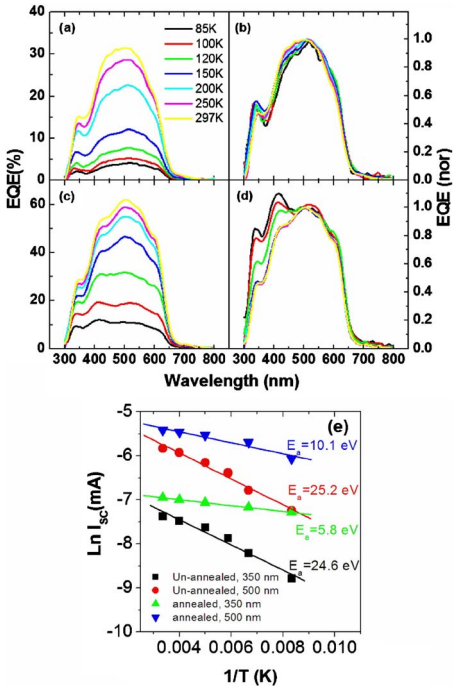

FIG. 2. (Color online) External quantum efficiency (EQE) spectra of (a) unannealed and (c) annealed P3HT:PCBM BHJ PVs at different temperatures and their normalized spectra of (b) unannealed and (d) annealed one. (e) The obtained E_a values of annealed and unannealed P3HT:PCBM BHJ PV devices from the different excitation wavelengths.

hopping conduction is reduced at low temperatures, leading to higher internal resistances and lower power production by the devices. For the unannealed device the main absorption features (PCBM, located at around 350 nm, and that of the P3HT, located at around 500 nm) respond in a similar way, implying that hopping is playing a significant role for both features. However, for the annealed device, the 350 and 500 nm features respond quite differently as a function of temperature. Specifically, the ratio of the power generated at 350 nm to that produced at 500 nm increases as temperature is reduced. We interpret this to mean that thermal activation within the PCBM phase for the conduction of the electrons has been reduced relative to that of the P3HT host.

When transport of uncharged excitons or charged polarons (after exciton separation) is dominated by hopping mechanisms, an activation energy E_a for hopping can be associated with the process. E_a can be determined directly from the temperature measurements for annealed (PV-H) and unannealed (PV-NH) PV devices, by plotting $\ln(J_{sc})$ vs $1/T$ from $J_{sc}=J_0 \exp(-E_a/kT)$. Figure 2(e) shows the obtained E_a values of PV-H and PV-NH from the different excitation wavelengths. We denote the E_a value for annealed devices obtained from 350 and 500 nm excitations as E_a (PV-H, 350) and E_a (PV-H, 500), respectively. E_a for unannealed devices obtained from 350 and 500 nm excitations is denoted as E_a (PV-NH, 350) and E_a (PV-NH, 500), respectively.

We note that from Eq. (1), E_a involves several processes including migration of the neutral exciton, dissociation at the heterojunction interface, transport of charged polaron, and charge transfer at the contacts. All of these involve hopping and we view E_a as a composite of the energies for all of these processes. However, since the PCBM in the unannealed device is homogeneously dispersed in the P3HT film, the exciton migration to the PCBM/P3HT interface does not

strongly influence the E_a value. Further, exciton dissociation through charge transfer at the P3HT/PCBM interface happens fast and efficiently, so it too does not strongly influence E_a.[13] Therefore, it is thought that the larger E_a values for unannealed PV devices are related to inefficient charge transport [steps (7) and (8)]. This is likely due to the lower crystallinity of the polymer coupled with possible scattering of the positive (hole)/negative (electron) carriers by the acceptor (PCBM)/donor (P3HT) phase, respectively.

In the annealed devices such simplifying assumptions cannot be made. Specifically, while we expect the hopping at the heterojunctions and at the contacts to be similar, between the annealed and unannealed devices, the polaron and exciton mobilities will certainly change as the system becomes crystalline. Therefore, the E_a values of the annealed devices reflect a change in neutral exciton mobility and in charge carrier transport to the electrode. However, since annealing will presumably result in increased neutral exciton mobility, E_a in these systems, as determined here, can be viewed as an upper limit on the charged polaronic mobility.

Comparing the annealed and unannealed systems we observe that E_a (PV-H, 350) and E_a (PV-H, 500) are lower than E_a (PV-NH, 350) and E_a (PV-NH, 500). Further, E_a (PV-H, 350) is lower than E_a (PV-H, 500), whereas E_a (PV-NH, 350) and E_a (PV-NH, 500) are similar. Thus, charged carrier transport in the bulk heterojunction system before annealing is similar for holes and electrons. In the annealed devices, by comparison charge carriers are transported through crystalline nanodomains of PCBM and crystalline polymer. These act as efficient charge transport paths with relatively high mobility. The result is a striking decrease in the activation of hopping processes, E_a values, in the annealed device.

These results lead to an important predictive result as stated by Markov *et al.*[12] By optimizing carrier mobility in this way, we can now utilize thicker films and allow for greater overall photoabsorption. From our previous report using metal nanoparticle doped PVs, we show that higher carrier mobility PV devices have maximum efficiencies at thicker active layers.[14] This simple result is frequently stated but rarely realized because the carrier mobilities in BHJ systems tend to be hardly increase in a balanced manner. However, as we show here, even slight increases in the active layer thickness can increase performance when the morphology of the nanophase is controlled.

The D1 through D3 devices were tested using an AM1.5g standard (Oriel) operating with an illumination intensity of 100 mW/cm^2. Our system's solar mismatch factor of 10% was determined using a calibrated standard diode. We also independently compared our system against a NREL certified simulator. Current-voltage characteristics were collected using Keithley 236 source-measurement unit.

Figure 3 compares *I-V* characteristics of the annealed devices and an unannealed (D1) P3HT:PCBM BHJ device. The PV device efficiency is listed for each curve. Note that efficiencies of over 6.1% can be achieved after thermal annealing. The devices are fabricated under identical conditions and the spread in values is typical.

Figure 3 correlates device efficiency of the overall P3HT:PCBM film thickness. The thinnest films absorb too little light, in general, the thickest films have too high internal resistance or are not charge balanced. For these PCBM to P3HT ratios and annealing temperatures, the device D2 seems to be optimal.

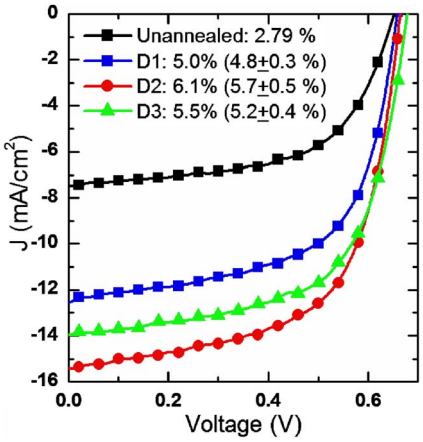

FIG. 3. (Color online) *I-V* characteristics of P3HT:PCBM BHJ PV with different P3HT:PCBM film thicknesses. The inset legend gives the efficiencies of the data graphs shown. The average over several devices is given in parentheses with the mean variation.

In conclusion, we have found that hopping mechanisms are modified in annealed BHJ systems to result in lower hopping activation energies. This is due to the formation of nanodomains within the morphology of the nanocomposite, allowing for improved charge mobility and charge balance. The result is that thicker films can be utilized in the high temperature annealed systems. At the optimum condition (device D2), we were able to achieve external power efficiencies of around 6.1%. This provides a significant step forward in the creation of polymer photovoltaics.

The authors thank AFOSR Grant No. FA9550-04-1-0161, the Korea Institute of Science and Technology (KIST) Contract Nos. 2E19590 and 2E19620, and the Korea Ministry of Information and Communication (MIC) for supporting this work.

[1] C. J. Brabec, N. S. Sariciftci, and J. C. Hummelen, Adv. Funct. Mater. **11**, 15 (2001).
[2] M. R. Reyes, K. Kim, and D. L. Carroll, Appl. Phys. Lett. **87**, 083506 (2005).
[3] W. L. Ma, C. Y. Yang, X. Gong, K. Lee, and A. J. Heeger, Adv. Funct. Mater. **15**, 1617 (2005).
[4] G. Li, V. Shrotriya, J. Huang, Y. Yao, T. Moriarty, K. Emery, and Y. Yang, Nat. Mater. **4**, 864 (2005).
[5] C. Yang, J. G. Hu, and A. J. Heeger, J. Am. Chem. Soc. **128**, 12007 (2006).
[6] C. Yang, F. P. Orfino, and S. Holdcroft, Macromolecules **29**, 6510 (1996).
[7] J. Geng and T. Zeng, J. Am. Chem. Soc. **128**, 16827 (2006).
[8] M. R. Reyes, K. Kim, J. Dewald, R. L. Sandoval, A. Avadhanula, S. Curran, and D. L. Carroll, Org. Lett. **7**, 5749 (2005).
[9] H. Heil, J. Steiger, S. Karg, M. Gastel, H. Ortner, H. von Seggern, and M. Stobel, J. Appl. Phys. **89**, 420 (2001).
[10] Y. Kim, S. Cook, S. M. Tuladhar, S. A. Choulis, J. Nelson, J. R. Durrant, D. D. C. Bradley, M. Giles, I. McCulloch, C. S. Ha, and M. Ree, Nat. Mater. **5**, 197 (2006).
[11] S. Goffri, C. Muller, N. S. Stutzmann, D. W. Breiby, C. P. Radano, J. Andreasen, R. Thompson, R. A. J. Janseen, M. M. Nielsen, P. Smith, and H. Sirringhaus, Nat. Mater. **5**, 950 (2006).
[12] D. E. Markov, J. C. Hummelen, P. W. M. Blom, and A. B. Sieval, Phys. Rev. B **72**, 045216 (2005).
[13] X. Ai, M. C. Beard, K. P. Knutsen, S. E. Shaheen, G. Rumbles, and R. J. Ellingson, J. Phys. Chem. B **110**, 25462 (2006).
[14] K. Kim and D. L. Carroll, Appl. Phys. Lett. **87**, 203113 (2005).